IOP Conf. Series: Journal of Physics: Conf. Series **828** (2017) 012019 doi:10.1088/1742-6596/828/1/012019

DM-induced frustration of the weakly coupled Heisenberg chains

Wen Jin and Oleg A. Starykh

Department of Physics and Astronomy, University of Utah, Salt Lake City, Utah 84112, USA

E-mail: wen.jin@utah.edu

Abstract. We present theoretical procedure for estimating interchain exchange coupling J' between antiferromagnetic spin-1/2 Heisenberg chains with frustration due to Dzyaloshinskii-Moriya (DM) interaction characterized by DM vectors $\mathbf{D}_y$ which are uniform within each chain y, but staggered between adjacent chains, $\mathbf{D}_y \sim (-1)^y \mathbf{D}$. Under a magnetic field $\mathbf{h} \parallel \mathbf{D}$ we obtain a field-temperature phase diagram which favorably agrees with the one experimentally observed. We then apply chain mean-field (CMF) technique to calculate interchain exchange J' from the critical field h_c at which the transition between the collinear spin-density wave and the cone states takes place. The CMF calculations are found to provide good physical description of the experimental measurements for the wide range of D/J'.

1. Introduction

Many experimental realizations of Heisenberg spin chain materials have become available over recent years. Here we present comparative analysis of two new interesting materials – $K_2CuSO_4Cl_2$ and $K_2CuSO_4Br_2$ [1, 2] – which represent an interesting and novel case of Heisenberg spin chains with *uniform* Dzyaloshinskii-Moriya (DM) interactions.

Both materials are believed to be described by the Hamiltonian (1) below and are characterized by a different set of parameters (J, D, J'), where J is the dominant intra-chain exchange, D is the DM interaction strength and J' is the interchain spin exchange. Despite close structural similarity, the two materials are characterized by different $h - T$ phase diagrams, as has been established by experiments in Prof. Zheludev's group in ETH [1–3]. That difference is attributed to the different D/J' ratio – according to Ref. [1] DM interaction is relatively weak in $K_2CuSO_4Cl_2$, so that $D/J' \sim 1$, while $K_2CuSO_4Br_2$ can be characterized as a strong DM material with $D/J' \sim 10$.

As we describe below and show in more details elsewhere [4], large D/J' ratio places Br-based material into a novel category of materials where interchain interaction between spins from adjacent chains is strongly frustrated by the uniform in-chain, but staggered between chains, DM interaction. This unique geometry of DM interactions makes $K_2CuSO_4Br_2$ somewhat similar to the honeycomb iridates family Li_2IrO_3 an incommensurate magnetic order of which is characterized by unusual counter-rotating spirals on neighboring sublattices [5]. This kind of frustration requires theoretical re-evaluation of the kind and mechanism of the eventual two- (or, three-) dimensional magnetic order that develops in the system at sufficiently low temperature. Our work provides such an analysis.

A variety of experimental techniques has been employed to characterize the parameters of $K_2CuSO_4Cl_2$ and $K_2CuSO_4Br_2$ [1, 2]. The dominant intra-chain exchange J has been estimated using the empirical fitting function of Ref. [6] to fit the uniform magnetic susceptibility data as well as by fitting the inelastic neutron scattering continuum, a unique feature of the Heisenberg spin-1/2 chain, to the Müller ansatz [7]. DM vector $\mathbf{D}$ has been measured by electron spin resonance (ESR) [2, 8]. However the interchain exchange interaction J' has been estimated from the chain mean-field theory fit based on Monte-Carlo improved study in Ref. [9]. This fit, however, completely neglects crucial for understanding of these materials DM interactions and moreover assumes that spin chains form simple non-frustrated cubic structure. The second assumption is not justified as well. Inelastic neutron scattering data show that the interchain exchange between spin chains in the $a-b$ plane is at least an order of magnitude stronger than that along the c-axis, connecting different $a-b$ planes. As a result, it is more appropriate to consider the current problem as two-dimensional whereby spin chains, running along the a-axis, interact weakly via $J' \ll J$ directed along the b-axis.

This is the geometry assumed in the present work. Using bosonization technique, we account for the intra-chain DM interaction non-perturbatively, and describe the competition between the cone and the longitudinal spin-density wave (SDW) orders. The interchain J' is estimated from the value of the zero-field critical temperature T_c, which is calculated with the help of the chain mean field (CMF) approximation [10]. The obtained T_c's are found to be in a good agreement with experimental measurements.

2. Hamiltonian

We consider weakly coupled antiferromagnetic Heisenberg spin-1/2 chains subject to a uniform Dzyaloshinskii-Moriya (DM) interaction and an external magnetic field. The system is described by the following Hamiltonian,

$$\mathcal{H} = \sum_{x,y}[J\mathbf{S}_{x,y}\cdot\mathbf{S}_{x+1,y} + J'\mathbf{S}_{x,y}\cdot\mathbf{S}_{x,y+1}] + \mathbf{D}\cdot\sum_{x,y}(-1)^y\mathbf{S}_{x,y}\times\mathbf{S}_{x+1,y} - h\cdot\sum_{x,y}S^z_{x,y}, \qquad (1)$$

where $\mathbf{S}_{x,y}$ is the spin-1/2 operator at site (x, y). J and J' denote isotropic intra- and inter-chain antiferromagnetic exchange couplings as shown in Fig. 1, and we account for interactions between nearest neighbors only. The inter-chain exchange is weak, of the order of $J' \sim 10^{-2}J$. DM interaction is parameterized by the DM vector $\mathbf{D} = D\hat{z}$, direction of which is staggered (note the factor $(-1)^y$) between adjacent chains. Importantly, vector $\mathbf{D}$ is uniform within a given y-th chain. $h = g\mu_B B$ is an external magnetic field along DM interaction.

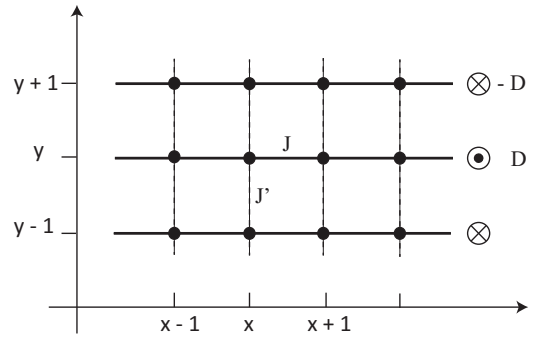

Figure 1. Sites, exchange couplings and DM vectors on coupled spin chains. Intra-chain bonds J (thick lines along $\hat{x}$), inter-chain bonds J' (dashed lines along $\hat{y}$), and $J' \ll J$. DM vectors on neighboring chain have opposite direction, either point into or out off paper.

2.1. Bosonization

In the low-energy continuum limit, Hamiltonian is expressed by bosonization [11–13],

$$\mathcal{H}_{\rm chain} = \tilde{\mathcal{H}}_0 + \tilde{\mathcal{H}}_{\rm bs} + \tilde{\mathcal{H}}_{\rm inter}, \qquad (2)$$

where $\tilde{\mathcal{H}}_0$ has quadratic form in terms of abelian bosonic fields ϕ, θ (see details in Appendix A), the Zeeman and DM interaction terms are absorbed in $\tilde{\mathcal{H}}_0$ by linear shifts of fields ϕ and θ, correspondingly. The harmonic Hamiltonian is perturbed by chain backscattering $\tilde{\mathcal{H}}_{\rm bs}$ and inter-chain $\tilde{\mathcal{H}}_{\rm inter}$ interactions, which read

$$\tilde{\mathcal{H}}_{\rm bs} = \int dx \Big\{ \pi v y_B (J_R^+ J_L^- e^{-i2t_\phi x} + \text{h.c.}) + 2\pi v y_z J_R^z J_R^z \Big\},\ t_\phi \equiv h/v, \tag{3}$$

and $\tilde{\mathcal{H}}_{\rm inter} = \mathcal{H}_{\rm cone} + \mathcal{H}_{\rm sdw}$, where

$$\mathcal{H}_{\rm cone} = c_1 \int dx \cos[\beta(\theta_y - \theta_{y+1}) + 2(-1)^y t_\theta x], \quad \mathcal{H}_{\rm sdw} = c_2 \int dx \cos[\frac{2\pi}{\beta}(\phi_y - \phi_{y+1})]. \tag{4}$$

The coupling constants are,

$$c_1 = J' A_3^2, \quad c_2 = J' A_1^2/2. \tag{5}$$

$v \simeq J\pi a/2$ is the spin velocity, a is lattice constant and $t_\theta \equiv D/v$. $\mathbf{J}_L(x)$ and $\mathbf{J}_R(x)$, are the uniform left and right spin currents, which are defined in Appendix A. The parameter $\beta = 2\pi R$ is related to the "compactification radius" R in the sine-Gordon (SG) model. In the absence of external field, the SU(2) invariant Heisenberg chain has $2\pi R^2 = 1$. The amplitudes A_1 and A_3 have been determined numerically [14]. $\mathcal{H}_{\rm cone}$ and $\mathcal{H}_{\rm sdw}$ are the transverse and longitudinal (with respect to the z-axis) components of inter-chain interaction respectively.

Table 1. Exchange constants for $K_2CuSO_4Cl_2$ and $K_2CuSO_4Br_2$: The intrachain exchange J is obtained by thermodynamic and neutron measurements. D values are from ESR measurements. Inter-chain exchange J' in fourth column is obtained by fitting data to Ref. [9]; inter-chain exchange $\mathcal{J}'$ in the last column is obtained by fitting data to our CMF calculation in Eq. (7), (9) and (10).

	J	D	J' by Ref. [9]	$\mathcal{J}'$ by CMF
$K_2CuSO_4Cl_2$	3.1 K	~ 0.04 K	0.031 K	0.073 K
$K_2CuSO_4Br_2$	20.5 K	0.28 K	0.034 K	0.20 K

2.2. Two phase diagrams

We notice that there is a position dependent oscillation term in $\mathcal{H}_{\rm cone}$ (4). The physical meaning is that staggered DM interaction forces spins in neighboring chains to rotate in opposite direction thereby frustrating the transverse inter-chain interaction. If the DM interaction is weak, $D \ll J'$ (the case of $K_2CuSO_4Cl_2$), oscillation in $\mathcal{H}_{\rm cone}$ is slow and does not affect renormalization group (RG) flow of the coupling constant c_1. One finds that in the presence of external magnetic field the more relevant $\mathcal{H}_{\rm cone}$ dominates over the $\mathcal{H}_{\rm sdw}$ and the ground state is cone state. Minimization of the argument of cosine in $\mathcal{H}_{\rm cone}$ has the effect of undoing the shift (A.9), resulting in a *commensurate cone* configuration shown in Fig. B1. The temperature-field phase diagram for this case is shown in Fig. 3.

If the DM interaction is strong, $D \gg J'$ (the case of $K_2CuSO_4Br_2$), $\mathcal{H}_{\rm cone}$ oscillates rapidly and averages to zero. As a result, the only inter-chain interaction that survives in this situation is the $\mathcal{H}_{\rm sdw}$, which promotes incommensurate longitudinal SDW order. However, a cone-like interaction between more distant chains can be generated by quantum fluctuations at low

energies [15]. The simplest of such interactions is given by the transverse interaction between the *next-neighbor* (NN) chains $\mathcal{H}_{\rm NN}$ (derivation of this term is presented in Ref. [4]),

$$\mathcal{H}_{\rm NN} = -c_3 \int dx \cos[\beta(\theta_y - \theta_{y+2})], \quad c_3 = \frac{\pi}{4}\frac{J'^2}{D} A_3^4 t_\theta^{2\Delta_1 - 1} \frac{\Gamma(1-\Delta_1)}{\Gamma(\Delta_1)}, \tag{6}$$

where $\Delta_1 \simeq 1/2$ at low fields. This is an indirect exchange, mediated by an intermediate chain $(y+1)$, and therefore its exchange coupling is rather weak, $(J')^2/D \ll J'$. Importantly this interaction is not frustrated (spins in chains y and $y+2$ are rotating in the *same* direction) and becomes more relevant with increasing magnetic field. $\mathcal{H}_{\rm NN}$ competes with $\mathcal{H}_{\rm sdw}$, and results in a phase transition from SDW to coneNN, a *cone-like incommensurate order* induced by $\mathcal{H}_{\rm NN}$, at some critical field h_c. For $K_2CuSO_4Br_2$ it appears that $h_c \approx 0.1$ T [1]. This coneNN order corresponds to $\theta_y - \theta_{y+2} = 2\pi/\beta$, and the resulting spiral spin configuration is illustrated in Fig. 2. The main role of DM interaction is to induce incommensurability, $\propto D/v$, in the *counter-rotating* spiral orderings in the neighboring spin chains, see Appendix B for more details.

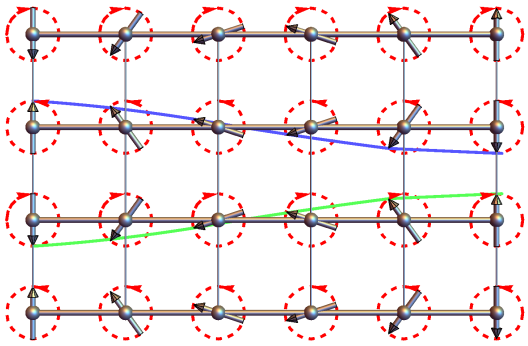

Figure 2. Staggered magnetization of the coneNN state, illustrated for a field $\mathbf{h} \parallel \mathbf{D}$, where all spins are ordered in the transverse plane. Red circles with arrows indicates the procession direction of spins, as one moves along each chain. Note that the arrows' direction alternates between consecutive chains, owing to the staggering of the DM vector. Blue and green curves illustrate spin orientation in neighboring chains.

3. Chain mean field calculation

The chain mean-field (CMF) approximation [10] allows one to calculate critical temperatures for different possible instabilities desribed in Sec. 2.2. There are three states that need to be considered, and we present the critical temperature for each state in the following. Details of the calculations can be found in Ref. [10] and Appendix C.

3.1. Cone order

Ordering temperature for the cone state $T_{\rm cone}$ is the solution of equation,

$$1 = \eta_1 (2\pi T_{\rm cone}/v)^{2\Delta_1 - 2} \frac{\Gamma(1-\Delta_1)}{\Gamma(\Delta_1)} |\Gamma(\Delta_1/2 + iy)|^4 \big[\cosh(2\pi y) - \cos(\pi\Delta_1)\big], \tag{7}$$

with

$$y = \frac{t_\theta v}{4\pi T_{\rm cone}}, \quad \eta_1 = \frac{c_1}{2\pi v}. \tag{8}$$

Δ_1 is the scaling dimension of N^+, its value in the limits of zero and full magnetization is shown in Table 2. The plot of $T_{\rm cone}$ for $K_2CuSO_4Cl_2$ is shown as the blue curve in Fig. 3 – this corresponds to Fig. 14 in Ref. [1]. Here we took the exchange constants $J = 3.1$ K and $D = 0.04$ K from Table 1. By fitting the zero-field experimental value of $T_{\rm cone}$ ($T_{\rm cone}|_{h=0}$ =77 mK in Ref. [1]) to Eq. (7), where $\Delta_1 = 1/2$, we obtain $\mathcal{J}'_{\rm Cl} = 0.073$ K. The (approximately) factor of 2 difference between our result and the previous estimate in Ref. [1] is caused by the

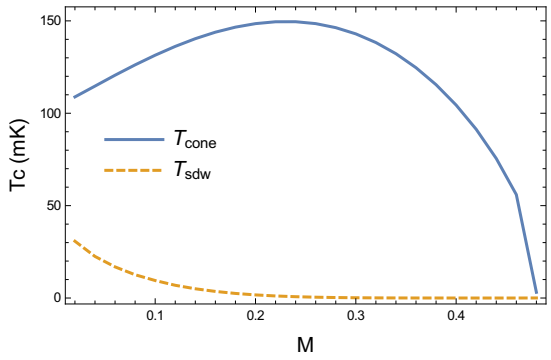

Figure 3. Critical temperatures of SDW ($T_{\rm sdw}$, orange dashed line) and cone ($T_{\rm cone}$, blue solid) as a function of magnetization M for $K_2CuSO_4Cl_2$, with $J = 3.1$ K, $D = 0.04$ K in Table 1 and $\mathcal{J}'_{\rm Cl} = 0.073$ K from Eq. (7) by setting $T_{\rm cone}|_{h=0}$ to 77 mK. The order with the larger critical temperature is the one realized. Here the phase diagram consists of a single cone phase.

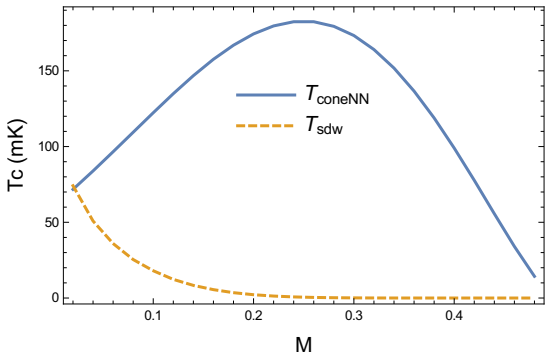

Figure 4. Critical temperatures of SDW ($T_{\rm sdw}$, orange dashed line) and coneNN ($T_{\rm coneNN}$, blue solid line) as a function of magnetization M for $K_2CuSO_4Br_2$, with $J = 20.5$ K, $D = 0.28$ K are taken from Table 1 , and $\mathcal{J}'_{\rm Br} = 0.20$ K from critical field $B_c \sim 0.1$ T (details in Sec. 4). Two curves intersect at very low field, indicating a SDW-coneNN phase transition.

accepted here two-dimensional geometry of the system, as described in the Introduction. Fig. 3 shows that $T_{\rm cone}$ is enhanced by field, and has a max close to 150 mK, which agrees well with the experimental maximum of $T_{\rm cone}$, see Fig. 14 in Ref. [1]. At high magnetic field $T_{\rm cone}$ starts to decrease because orthogonal to the magnetic field spin projection (the amplitude A_3 in (5)) decreases to zero on approaching the fully polarized phase.

Importantly, increasing the ratio D/J' suppresses $T_{\rm cone}$, until at some critical value $D_c/J' \approx 1.2$, the solution of Eq. (7) disappears completely. Mathematically, this value is determined by the maximum of the right-hand-side of Eq. (7) as a function of y [4]. Physically, strong DM interaction ($D/J' \gg 1$) frustrates transverse interchain coupling, effectively turning it off. As a result, the cone order is destroyed.

3.2. SDW order

The ordering temperature for SDW state is,

$$T_{\rm sdw} = \frac{v}{2\pi}\Big[\eta_2 \frac{\Gamma(1-\Delta_2)\Gamma(\Delta_2/2)^2}{\Gamma(\Delta_2)\Gamma(1-\Delta_2/2)^2}\Big/\Big(1+\eta_2\frac{\Gamma(\Delta_2-1/2)}{\sqrt{\pi}(1-\Delta_2)\Gamma(\Delta_2)}\Big)\Big]^{1/(2-2\Delta_2)}, \qquad (9)$$

with $\eta_2 = \pi c_2/v$. The denominator compensates the non-physical divergence which occurs when $\Delta_2 \to 1$ near the saturation transition, see Table 2. Calculated $T_{\rm sdw}$ for $K_2CuSO_4Cl_2$ and $K_2CuSO_4Br_2$ are shown in orange in Fig. 3 and Fig. 4, respectively. In Fig. 3, $T_{\rm sdw}$ is smaller than $T_{\rm cone}$, so that SDW does not realize. However, in Fig. 4, $T_{\rm sdw}$ is dominant at small fields $h < h_c$. At higher h (higher magnetization M) $T_{\rm coneNN}$ takes over, corresponding to the SDW-coneNN phase transition.

3.3. ConeNN

When it comes to coneNN state, its ordering temperature has a simple form, due to the fact that $\mathcal{H}_{\rm NN}$ is free from oscillation and $T_{\rm coneNN}$ is free from divergence ($\Delta_1 \leq 1/2$),

$$T_{\rm coneNN} = \frac{v}{2\pi}\Big[\eta_3 \frac{\Gamma(1-\Delta_1)\Gamma(\Delta_1/2)^2}{\Gamma(\Delta_1)\Gamma(1-\Delta_1/2)^2}\Big]^{1/(2-2\Delta_1)}, \tag{10}$$

with $\eta_3 = \pi c_3/v$. $T_{\rm coneNN}$ for $K_2CuSO_4Br_2$ is shown in Fig. 4, where values for J and D are from Table 1. $\mathcal{J}'_{\rm Br} = 0.20$ K is obtained from the calculation in Sec. 4, where we describe that for strong DM interaction the value of the interchain exchange $\mathcal{J}'$ can be obtained directly from the transition field h_c.

Table 2. Scaling dimensions $\Delta_{1/2}$ of transverse ($N^{\pm}$) and longitudinal (N^z) components of staggered magnetization $\mathbf{N}$ at magnetization M. The last two columns are the scaling dimensions in the limit of zero and full polarization, respectively.

	Operator	Field	Expression	$M=0$	$M=1/2$
Δ_1	$N^{\pm}$	θ	πR^2	1/2	1/4
Δ_2	N^z	ϕ	π/β^2	1/2	1

4. Determination of $\mathcal{J}'$ from the critical field h_c for strong DM interaction

Experiments on $K_2CuSO_4Br_2$ have observed phase transition at a very small magnetic field $B_c \sim 0.1$ T [1, 2]. This corresponds to a critical field $h_c = 0.1343$ K (with $h_c = g\mu_B B_c$, and set $\mu_0 = 1$). Clearly $h_c \ll J$, which is consistent with our low-field consideration. Using field-theoretical expression for the low-field magnetization, per site, $m(h)$ of the spin-1/2 Heisenberg chain [16]

$$m \to \frac{h}{2\pi v}[1 + \frac{1}{2\ln(J/h)}], \tag{11}$$

then we can estimate the critical magnetization $m_c \simeq 7.29 \times 10^{-4}$ at h_c. Here, spin wave $v = \pi J/2$, and the predominant exchange $J = 20.5$ K. Scaling dimensions of operators N^+ and N^z are Δ_1 and Δ_2, respectively, with $\Delta_1 = \pi R^2$, $\Delta_2 = \pi/\beta^2$. In the limit of small magnetization, the parameter $2\pi R^2$ is well fitted [10] by

$$2\pi R^2 = 1 - \frac{1}{2\ln(M_0/m)}, \tag{12}$$

where $M_0 = \sqrt{8/(\pi e)}$. Therefore, the two scaling dimensions are modified by the magnetization in opposite ways,

$$\Delta_1 = \frac{1}{2}[1 - \frac{1}{2\ln(M_0/m)}], \quad \Delta_2 = \frac{1}{2[1 - \frac{1}{2\ln(M_0/m)}]}. \tag{13}$$

These relations are illustrated in Fig. 6.

We now use ordering temperatures of the two competing orders, $T_{\rm sdw}(\Delta_2, J'/J)$ in Eq. (9) and $T_{\rm coneNN}(\Delta_1, J'/J)$ in Eq. (10), together with Eq. (13) and experimental value of m_c in order to find the ratio $J_p = J'/J$. The critical magnetization m_c satisfies the condition,

$$T_{\rm sdw}(m_c, J_p) = T_{\rm coneNN}(m_c, J_p). \tag{14}$$

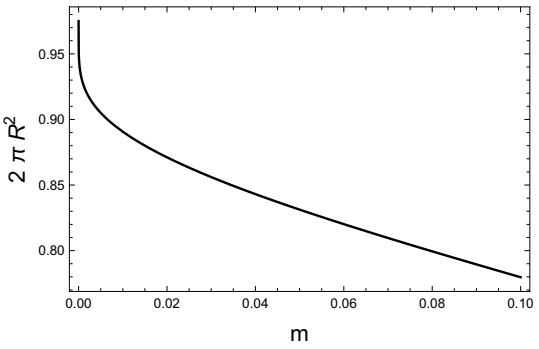

Figure 5. Parameter $2\pi R^2$ as a function of magnetization m, in the limit of small m, illustrating Eq. (12).

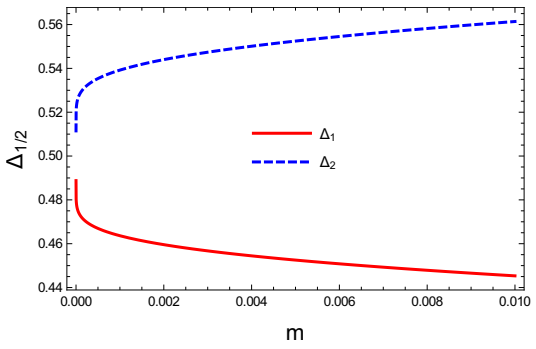

Figure 6. Two scaling dimensions $\Delta_{1/2}$ as a function of magnetization m, in the limit of small m, illustrating Eq. (13).

Fig. 7 shows that in the vicinity of the m_c, which is denoted by the red dot in the plot, J_p varies linearly with magnetization m. We find $J_p = 0.01024$, which results in the inter-chain exchange $\mathcal{J}'_{\rm Br} \approx 0.2$ K. The curves for $T_{\rm sdw}$ and $T_{\rm coneNN}$ intersect at $T_0 \equiv T_{\rm sdw}(m_c, \mathcal{J}'_{\rm Br}) = T_{\rm coneNN}(m_c, \mathcal{J}'_{\rm Br}) \simeq 77$ mK.

With $\mathcal{J}'_{\rm Br} = 0.2$ K, we compute the zero field ordering temperature of SDW order, $T_{\rm sdw}|_{h=0} \approx 112.12$ mK, which agrees with the zero field specific heat anomaly at 100 mK [1].

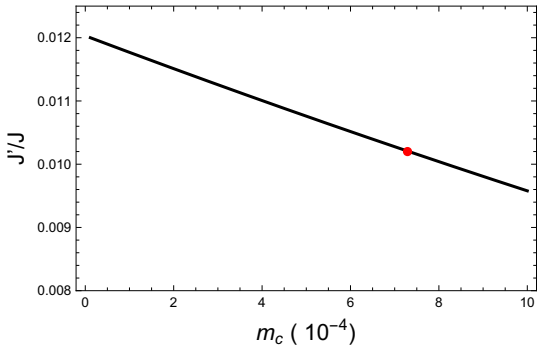

Figure 7. Relation between ratio $J_p = J'/J$ and magnetization m near m_c. The coordinate of the red dot is $(m_c, J_p) = (7.29, 0.01024)$, which gives the inter-chain exchange for $K_2CuSO_4Br_2$ as $\mathcal{J}'_{\rm Br} \approx 0.2$ K.

5. Order parameters at $T = 0$

Here we propose to study the magnetic orders in more details by calculating the associate order parameters, even though experimental attempts to measure them, via neutron scattering and muon-spin spectroscopy, remain inconclusive for now [3]. The spin configuration is determined by the relative ordering of θ (for cone and coneNN states) and ϕ (for SDW) phases on neighboring chains, as well as by the magnitude of the local staggered magnetization, Ψ. The former is described in Appendix B, while the latter is calculated in Appendix D. For example, commensurate cone state is characterized by

$$\mathbf{S}_{\mathbf{x},\mathbf{y}} = (0, 0, M) + (-1)^{x+y}|\Psi_{\rm cone}|(-\sin[\theta_0],\ \cos[\theta_0],\ 0). \tag{15}$$

The results of calculation in Appendix D are presented in Fig. 8 and 9. Comparing the two figures, we notice the order parameter has smaller magnitude in Br-compound, due to the stronger DM interaction which frustrates the system more. Also, cone-like orders are enhanced by magnetic field, while SDW order is monotonically suppressed by it.

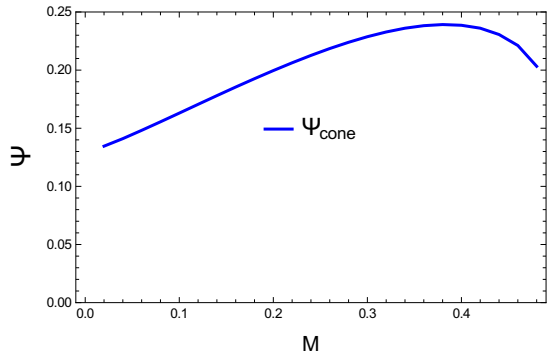

Figure 8. Order parameter of cone (Ψ_{cone}, blue) in $K_2CuSO_4Cl_2$, where $J'/J = 0.024$ and $D/J' = 0.55$, and Ψ_{cone} is enhanced by field.

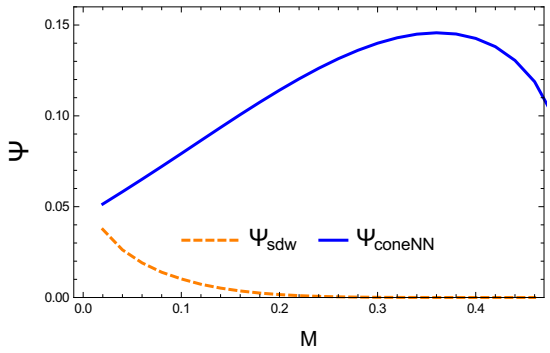

Figure 9. Order parameters of SDW (Ψ_{sdw}, orange dashed line) and coneNN (Ψ_{coneNN}, blue) in Br-compound, where $J'/J = 0.01$ and $D/J' = 1.4$.

6. Conclusion

We have studied effect of weak exchange J' between antiferromagnetic Heisenberg spin-1/2 chains on the phase diagrams of quasi-one-dimensional materials $K_2CuSO_4Cl_2$ and $K_2CuSO_4Br_2$ [1, 2], subject to the uniform but *staggered between chains* Dzyaloshinskii-Moriya (DM) interaction and external magnetic field. With the help of chain mean field calculation, J' can be determined quantitatively, and our results, denoted by $\mathcal{J}'$, are summarized in Table 1. For spin chains with strong DM interaction ($K_2CuSO_4Br_2$), one can extract value of J' directly from the critical field corresponding to the phase transition between the spin density wave to the coneNN states. The order parameter at zero temperature for each state is calculated as well.

Acknowledgments

We would like to thank A. Zheludev, M. Hälg and K. Povarov for detailed discussions of the experiments. This work was supported by the award from the National Science Foundation NSF DMR-1507054.

Appendix A. Bosonization

In the low-energy continuum limit the spin operator is represented by [11],

$$\mathbf{S}(x) \to \mathbf{J}_L(x) + \mathbf{J}_R(x) + (-1)^{x/a}\mathbf{N}(x), \tag{A.1}$$

with a is the lattice spacing, and continuous space coordinate is introduced via $x = na$, with n an integer. $\mathbf{J}_L(x)$ and $\mathbf{J}_R(x)$, are the uniform left and right spin currents, and $\mathbf{N}(x)$ is the staggered magnetization. These fields can be conveniently expressed in terms of abelian bosonic fields (ϕ, θ),

$$J_R^+ = \frac{1}{2\pi a}e^{-i\sqrt{2\pi}(\phi-\theta)},\ J_L^+ = \frac{1}{2\pi a}e^{i\sqrt{2\pi}(\phi+\theta)},\ J_R^z = \frac{\partial_x\phi - \partial_x\theta}{2\sqrt{2\pi}},\ J_L^z = \frac{\partial_x\phi + \partial_x\theta}{2\sqrt{2\pi}}. \tag{A.2}$$

$$\mathbf{N}(x) = \Big(- A_3 \sin[\beta\theta],\ A_3 \cos[\beta\theta],\ -A_1 \sin[\frac{2\pi}{\beta}\phi]\Big). \tag{A.3}$$

Then Hamiltonian in Eq. (A.4) can be expressed,

$$\mathcal{H} = \sum_y [\mathcal{H}_0 + \mathcal{V} + \mathcal{H}_{\text{bs}} + \mathcal{H}_{\text{inter}}], \tag{A.4}$$

where,

$$\mathcal{H}_0 = \frac{2\pi v}{3}\int dx(\mathbf{J_R}\cdot\mathbf{J_R}+\mathbf{J_L}\cdot\mathbf{J_L}) = \frac{v}{2}\int dx[(\partial_x\phi)^2+(\partial_x\theta)^2], \tag{A.5}$$

$$\mathcal{V} = \mathcal{H}_{\rm Z}+\mathcal{H}_{\rm DM} = -h_z\int dx(J^z_R+J^z_L)+(-1)^y D\int dx(J^z_R-J^z_L), \tag{A.6}$$

$$\mathcal{H}_{\rm bs} = -g_{\rm bs}\int dx[J^x_RJ^x_L+J^y_RJ^y_L+(1+\lambda)J^z_RJ^z_L], \quad \mathcal{H}_{\rm inter} = J'\int dx\mathbf{N}_y\cdot\mathbf{N}_{y+1}, \tag{A.7}$$

where $v\simeq J\pi a/2$ is the spin velocity, $\lambda = c'D^2/J^2$ describes an Ising-like anisotropy induced by DM interaction [13]. $\mathcal{V}$ contains the last two terms of Eq. (1), it collects all vector-like perturbations of the bare chain Hamiltonian $\mathcal{H}_0$. $\mathcal{H}_Z$ and $\mathcal{H}_{\rm DM}$ are the Zeeman and DM interactions, respectively. $\mathcal{H}_{\rm bs}$ describes residual backscattering interaction between right- and left-moving spin modes of the chain, its coupling is estimated as $g_{\rm bs}\approx 0.23\times(2\pi v)$, see Ref. [13] for details. The constant $c' = (2\sqrt{2}v/g_{\rm bs})^2$ is about 3.83 from the Bethe ansatz solution, see (B2) in Ref. [13]. The inter-chain interaction is described by $\mathcal{H}_{\rm inter}$, in which we kept the most relevant, in renormalization group sense, contribution, $\mathbf{S}_{x,y}\cdot\mathbf{S}_{x,y+1}\to\mathbf{N}_{x,y}\cdot\mathbf{N}_{x,y+1}$. Evidently, the linear terms in $\mathcal{V}$ can be *absorbed* into $\mathcal{H}_0$ by shifting fields ϕ and θ appropriately,

$$\phi\to\phi+\frac{t_\phi}{\sqrt{2\pi}}x, \qquad t_\phi\equiv\frac{h}{v}, \tag{A.8}$$

$$\theta\to\theta+(-1)^y\frac{t_\theta}{\sqrt{2\pi}}x, \qquad t_\theta\equiv\frac{D}{v}. \tag{A.9}$$

As a result of the shifts, the spin currents and the staggered magnetization are modified as

$$J^+_R\to J^+_Re^{-i(t_\phi-t^y_\theta)x},\ J^+_L\to J^+_Le^{i(t_\phi+t^y_\theta)x},\ J^z_R\to J^z_R+\frac{(t_\phi-t^y_\theta)}{4\pi},\ J^z_L\to J^z_L+\frac{(t_\phi+t^y_\theta)}{4\pi}, \tag{A.10}$$

$$N^+\to N^+e^{it^y_\theta x}, \quad N^z\to -A_1\sin(\frac{2\pi}{\beta}\phi+t_\phi x). \tag{A.11}$$

Here $t^y_\theta\equiv(-1)^y t_\theta$ depends on the parity of the chain index y. Notice that the shift introduces oscillating position-dependent factors to transverse components of $\mathbf{J}$ and $\mathbf{N}$. The Hamiltonian now reads as Eq. (4). The complete form of $\mathcal{H}_{\rm sdw}$ is,

$$\begin{aligned}\mathcal{H}_{\rm sdw} &= J'A_1^2\int dx\sin[\frac{2\pi}{\beta}\phi_y+t_\phi x]\sin[\frac{2\pi}{\beta}\phi_{y+1}+t_\phi x]\\ &= \frac{1}{2}J'A_1^2\int dx\Big\{\cos[\frac{2\pi}{\beta}(\phi_y-\phi_{y+1})]-\cos[\frac{2\pi}{\beta}(\phi_y+\phi_{y+1})+2t_\phi x]\Big\}.\end{aligned} \tag{A.12}$$

The effect of position-dependent phase $t_\phi x$ is to induce sign-changing oscillations on the spatial scale $\propto 1/t_\phi\sim J/h$. The corresponding RG scale is $\ell_\phi\sim\ln(J/h)$. This needs to be compared with the RG scale $\ell_{\rm inter}\sim\ln(J/J')$ on which $\mathcal{H}_{\rm sdw}$ reaches strong coupling. For $\ell_{\rm inter}\ll\ell_\phi$ ($h\ll J'$) the oscillations are not important and SDW order is commensurate. In the opposite limit $\ell_{\rm inter}\gg\ell_\phi$ ($h\gg J'$) the oscillations are frequent and wash out the second term in (A.12). This corresponds to the development of incommensurate SDW. The commensurate-incommensurate change takes place at $h\sim J'$. Here we assume that magnetic field h_c, at which SDW-coneNN transition takes place (see Sec. 4), satisfies $h_c\geq J'$ condition and use the reduced form of $\mathcal{H}_{\rm sdw}$, first term in (A.12) and Eq. (4). The obtained estimate for the interchain $J'\approx 0.2$ K is found to be consistent with the made assumption.

Appendix B. Spin configurations

The spin operator has two parts,

$$\mathbf{S}_{\mathbf{x},\mathbf{y}} = \mathbf{M} + (-1)^x \mathbf{N}_y(x), \tag{B.1}$$

with $\mathbf{M}$ is magnetization along the magnetic field, and $\mathbf{N_y}(\mathbf{x})$ is the staggered magnetization on site (x, y). We have three competing interactions $\mathcal{H}_{\rm cone}$, $\mathcal{H}_{\rm sdw}$ and $\mathcal{H}_{\rm NN}$ as in Eq. (4) and (6). When the dominant interaction is $\mathcal{H}_{\rm cone}$, and the ground state is commensurate cone phase.

$$\mathbf{N}_y(x) = (-1)^y |\Psi_{\rm cone}|(-\sin[\theta_0],\ \cos[\theta_0],\ 0). \tag{B.2}$$

This cone order is illustrated in Fig. B1. When the most relevant interaction is $\mathcal{H}_{\rm sdw}$, the ground state is collinear SDW state. The system will be ordered in ϕ field, with $\phi_y = \phi_0 + \sqrt{\frac{\pi}{2}} y + \frac{hx}{\sqrt{2\pi}v}$, and staggered magnetization is

$$\mathbf{N}_y(x) = (-1)^y |\Psi_{\rm sdw}|(0,\ 0,\ \sin[\sqrt{2\pi}\phi_0 + \frac{hx}{v}]). \tag{B.3}$$

If $\mathcal{H}_{\rm NN}$ is the most relevant interchain interaction, we obtain cone-like order in the plane perpendicular to the external magnetic field, similar to $\mathcal{H}_{\rm cone}$ case. The order corresponds to $\theta_y = \theta_0 + (-1)^y \frac{Dx}{\sqrt{2\pi}v}$. (In principle, the constant phase θ_0 can be different for *even* and *odd* chains – it remains unclear how these two subsystems couple to each other in the regime of strong DM interaction.) As a result, the staggered magnetization reads

$$\mathbf{N}_y(x) = |\Psi_{\rm coneNN}|(-\sin[\sqrt{2\pi}\theta_0 + (-1)^y Dx/v],\ \cos[\sqrt{2\pi}\theta_0 + (-1)^y Dx/v],\ 0). \tag{B.4}$$

This order is shown in Fig.2. Different from order in (B.2), coneNN is spiraling in the transverse $x - y$ plane.

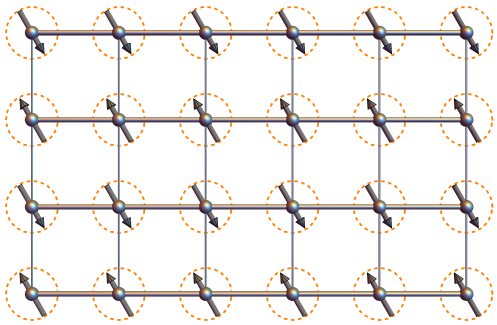

Figure B1. Staggered magnetization of the cone state, illustrated for a field $\mathbf{h} \parallel \mathbf{D}$, where all spins are ordered in the transverse plane. This order is commensurate. Spins pointing to opposite directions, reflecting the anti-ferromagnetic interaction between neighboring chains.

Appendix C. Chain mean field approximation

For an interaction,

$$\mathcal{H}_y = \mathcal{H}_0 - c \int dx \cos[\beta\theta_y] \cos[\beta\theta_{y+1}], \tag{C.1}$$

with the approximation of chain mean field(CMF), the spin (staggered magnetization part) takes an average value

$$\tilde{\psi} = \langle \cos[\beta\theta_y] \rangle. \tag{C.2}$$

Then the Hamiltonian (C.1) reduces to,

$$\mathcal{H}_y = \mathcal{H}_0 - 2c\tilde{\psi} \int dx \cos[\beta\theta_y], \tag{C.3}$$

where the factor of 2 arises from two neighboring chains. Eq. (C.3) is just the sine-Gordon Hamiltonian, to which three interchain interactions in Eq. (4) and (6) along with $\mathcal{H}_0$ in Eq. (A.5) can reduce. We can rearrange $\mathcal{H}_{\rm cone}$ in Eq. (4), by shifting the fields θ,

$$\theta_y \to \tilde{\theta}_y + (-1)^y \pi/(2\beta) - (-1)^y t_\theta x, \tag{C.4}$$

then $\mathcal{H}_{\rm cone}$ changes sign and transforms to,

$$\mathcal{H}_{\rm cone} = -2c_1\tilde{\psi}_1 \int dx \cos[\beta\tilde{\theta_y}], \tag{C.5}$$

with $\tilde{\psi}_1 = \langle\cos[\beta\tilde{\theta}]\rangle$ and $\cos\beta\tilde{\theta} \sim \cos[\beta\theta + (-1)^y t_\theta x]$ is the x-component of staggered magnetization in Eq. (A.11). Similar procedure (but shift is independent of position) can be applied to $\mathcal{H}_{\rm sdw}$ in Eq. (4) and $\mathcal{H}_{\rm NN}$ in Eq. (6),

$$\mathcal{H}_{\rm sdw} = -2c_2\tilde{\psi}_2 \int dx[\cos\frac{2\pi}{\beta}\phi_y], \quad \mathcal{H}_{\rm NN} = -2c_3\tilde{\psi}_3 \int dx \cos[\beta\theta_y], \tag{C.6}$$

where $\tilde{\psi}_2 = \langle\cos[2\pi\phi/\beta]\rangle$, $\tilde{\psi}_3 = \langle\cos[\beta\theta]\rangle$.

To determine the critical temperature, we can expand Eq. (C.3), with self-consistent condition,

$$\frac{1}{2c} = \chi(q=0,\omega_n=0;T_c) \quad = \int dx \int_0^{1/T_c} d\tau e^{iqx+\omega_n\tau}\langle O(x,\tau)O(0,0)\rangle_0 \tag{C.7}$$

$\chi(q,\omega_n;T)$ is momentum and frequency dependent susceptibility at finite temperature T. Here the operators in consideration are,

$$O = \cos(\sqrt{4\pi\Delta_1}\theta) \quad \text{or} \quad O = \cos(\sqrt{4\pi\Delta_2}\phi). \tag{C.8}$$

With two scaling dimensions in Table. 2, $\Delta_1 = \pi R^2$ and $\Delta_2 = \pi/\beta^2$. Here we follow the standard calculation in Ref. [10], where Eq. (D.55) gives the expression of static susceptibility,

$$\chi(q=0,\omega_n=0;T_c) = \frac{\pi u\alpha^2}{2}\Big[(2\pi T\alpha)^{2\Delta-2}\frac{\Gamma(1-\Delta)\Gamma(\Delta/2)^2}{\Gamma(\Delta)\Gamma(1-\Delta/2)^2} - \frac{\Gamma(\Delta-1/2)}{\sqrt{\pi}(1-\Delta)\Gamma(\Delta)}\Big]. \tag{C.9}$$

Here, Δ is either Δ_1 or Δ_2, and second term removes the non-physical divergence as Δ approaching to 1.

Appendix D. Order parameter at $T = 0$

For a sine-Gordon model in Eq. (C.3), its action

$$S_{\rm sG} = \int dxdy\Big(\frac{1}{2}(\partial_x\theta)^2 + \frac{1}{2}(\partial_y\theta)^2 - 2\mu\cos[\beta\theta]\Big). \tag{D.1}$$

here, $\mu = c\langle\cos[\beta\theta]\rangle/v$, and $\tau = y/v$. According to Ref. [10, 17], we have the expression for $\tilde{\psi} \equiv \langle\cos\beta\theta\rangle$ as a function of magnetization M,

$$\tilde{\psi}(M) = \Big[(\frac{c}{v})^{\beta'^2}\sigma'(M)^{1-\beta'^2}\Big]^{1/(1-2\beta'^2)}, \tag{D.2}$$

where $\beta' = \beta/\sqrt{8\pi}$, and

$$\sigma'(M) = \frac{\tan[\pi\xi/2]}{2\pi(1-\beta'^2)}\left[\frac{\Gamma(\frac{\xi}{2})}{\Gamma(\frac{1+\xi}{2})}\right]^2\Big[\frac{\pi\Gamma(1-\beta'^2)}{\Gamma(\beta'^2)}\Big]^{1/(1-\beta'^2)}, \quad \xi = \frac{\beta'^2}{1-\beta'^2} = \frac{\beta^2}{8\pi-\beta^2}, \tag{D.3}$$

Eq. (D.2) is a general form of order parameter for sine-Gordon model. The three interactions in consideration are Eq. (C.4) and (C.6), with $\beta = 2\pi R$, and their corresponding parameter β' are,

$$\beta'_{1/3} = \Delta_1/2, \quad \beta'_2 = \Delta_2/2, \tag{D.4}$$

where $\beta'_{1,2,3}$ are associated with $\tilde{\psi}_{1,2,3}$. Now we can compute the order parameters for two materials $K_2CuSO_4Cl_2$ and $K_2CuSO_4Br_2$ with their exchange constants in Table 1. For $K_2CuSO_4Cl_2$, there is single cone with order parameter,

$$\Psi_{\text{cone}} = A_3\Big[(\frac{c_1}{v})^{\Delta_1}\sigma'(M)^{2-\Delta_1}\Big]^{1/(2-2\Delta_1)}. \tag{D.5}$$

Ψ_{cone} is shown in Fig. 8. For $K_2CuSO_4Br_2$, two order parameters need to be considered,

$$\Psi_{\text{sdw}} = A_1\Big[(\frac{c_2}{v})^{\Delta_2}\sigma'(M)^{2-\Delta_2}\Big]^{1/(2-2\Delta_2)}, \quad \Psi_{\text{coneNN}} = A_3\Big[(\frac{c_3}{v})^{\Delta_1}\sigma'(M)^{2-\Delta_1}\Big]^{1/(2-2\Delta_1)} \tag{D.6}$$

and they are shown in Fig. 9.

References

[1] Hälg M, Lorenz W E A, Povarov K Y, Månsson M, Skourski Y and Zheludev A 2014 *Phys. Rev. B* **90**(17) 174413
[2] Smirnov A I, Soldatov T A, Povarov K Y, Hälg M, Lorenz W E A and Zheludev A 2015 *Phys. Rev. B* **92**(13) 134417
[3] Hälg M 2015 *Quantum criticality, universality and scaling in organometallic spin-chain compounds* Ph.D. thesis ETH-ZÃijrich
[4] Jin W and Starykh O A 2016 Phase diagram of weakly coupled heisenberg chains subject to a uniform dzyaloshinskii-moriya interaction *In preparation*
[5] Kimchi I and Coldea R 2016 *ArXiv e-prints* (*Preprint* `1606.05356`)
[6] Johnston D C, Kremer R K, Troyer M, Wang X, Klümper A, Bud'ko S L, Panchula A F and Canfield P C 2000 *Phys. Rev. B* **61**(14) 9558–9606
[7] Müller G, Thomas H, Beck H and Bonner J C 1981 *Phys. Rev. B* **24**(3) 1429–1467
[8] Povarov K Y, Smirnov A I, Starykh O A, Petrov S V and Shapiro A Y 2011 *Phys. Rev. Lett.* **107**(3) 037204
[9] Yasuda C, Todo S, Hukushima K, Alet F, Keller M, Troyer M and Takayama H 2005 *Phys. Rev. Lett.* **94**(21) 217201
[10] Starykh O A, Katsura H and Balents L 2010 *Phys. Rev. B* **82**(1) 014421
[11] Gangadharaiah S, Sun J and Starykh O A 2008 *Phys. Rev. B* **78**(5) 054436
[12] Schnyder A P, Starykh O A and Balents L 2008 *Phys. Rev. B* **78**(17) 174420
[13] Garate I and Affleck I 2010 *Phys. Rev. B* **81**(14) 144419
[14] Essler F H L, Furusaki A and Hikihara T 2003 *Phys. Rev. B* **68**(6) 064410
[15] Starykh O A and Balents L 2007 *Phys. Rev. Lett.* **98**(7) 077205
[16] Affleck I and Oshikawa M 1999 *Phys. Rev. B* **60**(2) 1038–1056
[17] Lukyanov S and Zamolodchikov A 1997 *Nuclear Physics B* **493**(3) 571 – 587